Multilayer Composite Surfaces Prepared by an Electrostatic Self-Assembly Technique with Quaternary Ammonium Salt and Poly(acrylic acid) on Poly(acrylonitrile-*co*-acrylic acid) Membranes

Takaomi Kobayashi,[1] Huitan Fu,[1] Qian Cui,[1,2] Hongying Wang[2]

[1]*Department of Materials Science and Technology, Nagaoka University of Technology, 1603-1 Kamitomioka, Nagaoka, Niigata 940-2188, Japan*
[2]*Material Engineering School, Zhengzhou University, Zhengzhou 450052, People's Republic of China*

Received 5 June 2007; accepted 2 June 2008
DOI 10.1002/app.28849
Published online 8 September 2008 in Wiley InterScience (www.interscience.wiley.com).

ABSTRACT: An electrostatic self-assembly technique was applied to prepare ion complex polymer layers on polyacrylonitrile with acrylic acid segments {poly(acrylonitrile-*co*-acrylic acid) [P(AN-*co*-AA)]}. For the ionic complex layers, quaternary ammonium salts, such as cetyl trimethyl ammonium chloride (CTAC) and tetramethyl ammonium chloride (TMAC), were used as cationic species, and also, poly(acrylic acid) (PAA) was used as an anionic species. These cationic and anionic species were self-assembled alternately on the surface of the P(AN-*co*-AA) membrane. Fourier transform infrared spectroscopy, AFM, and water contact angle measurements of the membrane surface were used to confirm the formation of the multilayer composites on the P(AN-*co*-AA). The permeabilities of water and macromolecules of different molecular weights were evaluated by a membrane filtration technique. The values of permeability strongly depended on the formation layer by layer of these ion composites on the base P(AN-*co*-AA). Through the measurement of the values of the contact angle of water, it was clear that surface nature of the base membrane treated by CTAC or TMAC and PAA dramatically changed. We concluded that such an electrostatic self-assembly technique is useful for the preparation of multicomposite layers to modify the surface of base P(AN-*co*-AA) membranes. © 2008 Wiley Periodicals, Inc. J Appl Polym Sci 110: 3234–3241, 2008

Key words: films; membranes; modification; surfaces

INTRODUCTION

For the preparation of composite membranes, dip coating, spray coating, and spin coating are common techniques in addition to interface polymerization, filling polymerization, and plasma polymerization on the surface of polymer membranes. However, such procedures are complicated, and the surface structures of the treated membranes are often uncontrollable. Multilayer composites made by electrostatic attraction is a technique for deposited molecules and nanoparticles to form thin composite layers on a solid substrate. Designated as an *electrostatic self-assembly* (ESA) technique, Decher and coworkers[1–4] proposed that such a technique easily makes composite layers with a nanohierarchy structure. For the preparation of polymer films with good thermal stability and mechanical performance, the ESA technique has been applied. Usually, the composite layer is formed by the electrostatic attraction of the opposite ions on the base polymer surface. Additionally, a low-cost and simple procedure is advantageous in addition to alternative surface modification by the formation of a simple ion complex layer on the base polymer surface. So far, studies of ESA multilayers have been carried out to separate membranes for gasses, ions, and liquids.[5–9] For example, self-assembled polyelectrolyte layers with nanostructured units on the base membrane were applied for solvent dehydration by pervaporation. The membrane material had good separation properties of isopropyl alcohol from a water mixture. Also, the composition layers of polyvinylammonium salt and poly(vinyl sulfate) were alternated by the formation of ESA layers, which was the main approach used to report uses of the composite membrane for a metal-ion complex as the transport target.[5] We followed the field of investigation for more background information about selective ion transports across self-assembled polyelectrolyte membranes and films.[10,11] It was reported that multilayers with self-assembled polyelectrolytes improved ethanol/water mixture[12–14] and self-assembled DNA composite

Correspondence to: T. Kobayashi (takaomi@nagaokaut.ac.jp).

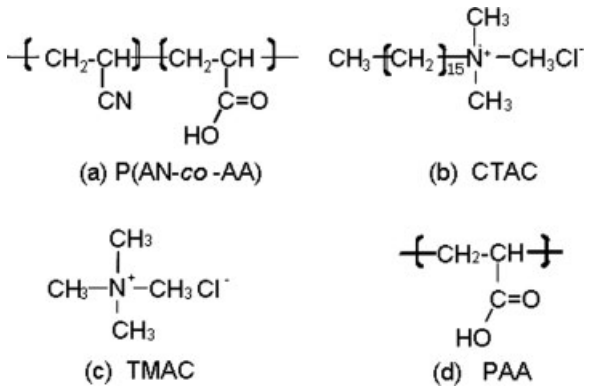

Scheme 1 Chemical structures of P(AN-*co*-AA), CTAC, TMAC, and PAA.

membranes.[15,16] However, there have still been few examples of the combination of such ion complexes to develop novel functionality with such alternative surface treatments on separation membranes. Because the approach of another alternating amphiphilic quaternary ammonium ion and polyanion has been limited in the ESA technique, such combinations seem to show a good opportunity to meet specific surface modification by the ESA technique for the functionality of separation membranes.

In an effort to develop a novel type of separation membrane, the purpose of this study was to adopt such an ESA technique to prepare alternative composite surfaces on the base membrane support. A polyacrylonitrile copolymer with acrylic acid (AA), poly(acrylonitrile-*co*-acrylic acid) [P(AN-*co*-AA); Scheme 1(a)], was used as the base membrane material. The quaternary ammonium salt was used as a cation to prepare the ESA multilayers of amphiphilic quaternary ammonium ions and polyanions on the P(AN-*co*-AA) membrane. The evidence showed that the properties of the alternative ion complex layers on the membrane surface were influenced by the amphiphilic nature of the quaternary ammonium salt used for the ESA technique.

EXPERIMENTAL

Materials

The base membrane material, P(AN-*co*-AA), was synthesized with acrylonitrile (AN) and AA monomers (AN/AA molar ratio = 90 : 10) by radical polymerization with dimethyl sulfoxide as the solvent and azobisisobutyronitrile as the initiator.[17] Here, AN was a membrane-formation segment and AA was a functional segment that provided negatively charged sites on the base membrane. Cetyl trimethyl ammonium chloride [CTAC; Scheme 1(b)] and tetramethyl ammonium chloride [TMAC; Scheme 1(c)] were used as cations to alternate with poly(acrylic acid) (PAA) anions [Scheme 1(d)]. The average molecular weight of the PAA (Nakarai, Tokyo) was 250,000. Poly(ethylene glycol) (PEG; Nakarai) was purchased with molecular weights of 1540, 10,000, and 20,000, and dextran had molecular weights of 6000, 70,000, 500,000, and 2,000,000. They were used without further purification for membrane filtration.

Preparation of the multilayer composite membranes

The base membrane made of P(AN-*co*-AA) was prepared by the phase-inversion method.[17] An aqueous solution with 10^{-2} *M* concentrations of CTAC, TMAC, and PAA was prepared and used for dipping solutions on the surface of the P(AN-*co*-AA) membrane. The water used was 18.2 $m\Omega/cm^{-1}$ (Millipore water) throughout whole experiment. The preparation procedure consisted of the following four steps: (1) immersion of the base membrane in the CTAC or TMAC solution (concentration = 1 g/L), (2) immersion of the membrane in pure water to wash out the excessive cation, (3) immersion in the PAA solution (concentration = 1 g/L), and then (4) immersion in pure water to wash out the excessive PAA anion. These steps were repeated to form multiple layers of CTAC and PAA by alternate deposition on the base P(AN-*co*-AA) (Scheme 2).

Measurements

Fourier transform infrared (FTIR) spectra of the P(AN-*co*-AA) without and with ESA treatment were measured with an FTIR spectrophotometer (IR Prestige-21, Shimadzu, Japan). The surface morphology of the treated P(AN-*co*-AA) was taken with an atom force microscope (Nanopics 1000s) with a dynamic force microscopy cantilever in contact mode. Image analyses were performed with supplied software (Data Analysis Program for Three Dimensions, Version 1.2, Seiko Instruments Inc., Japan). The contact angle of water of the treated surface was measured

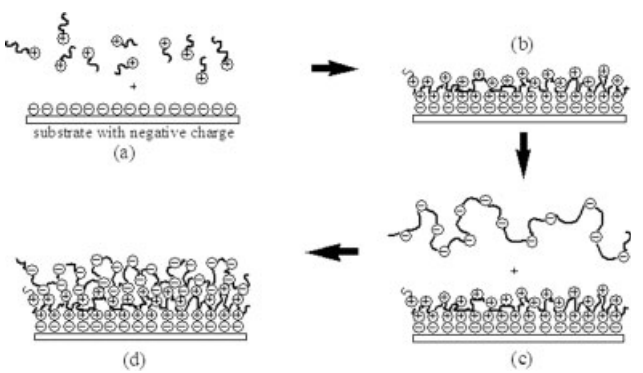

Scheme 2 Preparation procedure of the ESA multilayer on the polymer membrane with a negative charge.

TABLE I
Deposited Layer Amounts (mmol/g) of CTAC or TMAC and PAA on the Base Membrane by Each Cycle

Cycle	1	2	3	4	5	6
CTAC/PAA	1.4	1.4	1.3	1.5	1.4	1.4
TMAC/PAA	1.6	1.6	1.6	1.6	1.6	1.6

with a contact-angle goniometer at 25°C. The droplet view was observed, and the contact angles of water on the membranes could be read through the goniometer window. For each sample, four drops were analyzed, and the obtained values of the contact angles were of standard deviation. The droplet volume was about 2 μL for each measurement. In the filtration measurements, water flux and rejection were measured with PEG and dextran with an applied pressure of 0.4 kgf/cm^2 with ultrafiltration cell (Amicon 8010, 50-mL volume). The concentration of the PEG and dextran was 30 mg/L in aqueous solution.

RESULTS AND DISCUSSION

FTIR analyses of the multilayer composite polymers

As shown in Scheme 2, the ESA technique for CTAC/PAA would be applicable for different surface natures by the repetition of these alternating compositions. To estimate the deposited layers of CTAC and PAA on the base P(AN-*co*-AA) membrane, we determined the increase in the deposited weight of the CTAC or PAA layer by weighing the membrane. Table I lists the deposited layer amounts for CTAC or TMAC and PAA. The value of the deposited layer amount (mmol/g) was calculated as $\Delta m/F_w$, where Δm is the increment weight of the deposited layer and F_w is the molar mass, $F_w = 319$ and 72 g/mol for CTAC and PAA, respectively. The obtained values were approximately 1.4 mmol/g for the CTAC/PAA system and 1.6 mmol/g for the TMAC/PAA system. To confirm the chemical component of the deposited layer, FTIR spectroscopy was applied. Figure 1 shows the IR spectra of the base P(AN-*co*-AA), the P(AN-*co*-AA)/CTAC monolayer composite, and the P(AN-*co*-AA)/CTAC/PAA multilayer composite. Shown in Figure 1(c) is the spectrum of the base P(AN-*co*-AA). Figure 1 also shows the spectrum of the P(AN-*co*-AA)/CTAC monolayer [Fig. 1(d)] and the P(AN-*co*-AA)/CTAC/PAA [Fig. 1(e)], P(AN-*co*-AA)/CTAC/PAA/CTAC [Fig. 1(f)], and P(AN-*co*-AA)/CTAC/PAA/CTAC/PAA [Fig. 1(g)] composites. As shown in Figure 1(c), there was a wide and strong absorption peak near 3500–2800 cm^{-1}, which was assigned to the dimer formed by hydrogen bonds between the carboxylic acids of the AA segments of the P(AN-*co*-AA). Also, the dissociated carboxylic group was assigned as a characteristic absorption peak at 1645 cm^{-1}. As shown in Figure 1(d), the band peak for the hydrogen bond of a part of the dimer was reduced after CTAC was deposited on the surface of the base polymer. Thus, the absorption strength at 3500–2800 cm^{-1} became weak. In addition, the strong C—H absorption strength at 1454 cm^{-1} increased. The C=O absorption strength at 1737 cm^{-1} was somewhat lower than that of the —C≡N strength at 2300 cm^{-1}. This was because part of the carboxylic group dissociated to react with CTAC by electrostatic attraction.

Because of the electrostatic interaction between the CTAC and AA segments of the base P(AN-*co*-AA) and a second interaction between the CTAC and AA groups of PAA, the treated surface properties changed. To compare each IR spectra, the value of the ratios of the ⟩C=O bands at 1737 and 1654 cm^{-1} are shown in Figure 2. The band intensity of the ⟩C=O group decreased as the CTAC was deposited and increased as the was PAA deposited. Because a part of the carboxylic group of the AA segment associated electrostatically with CTAC after CTAC was deposited, the value of the ⟩C=O band intensity decreased with the formation of the CTAC layer between layer numbers 0 and 1 and increased after PAA was deposited between numbers 1 and 2. When the PAA layer was the top layer of the

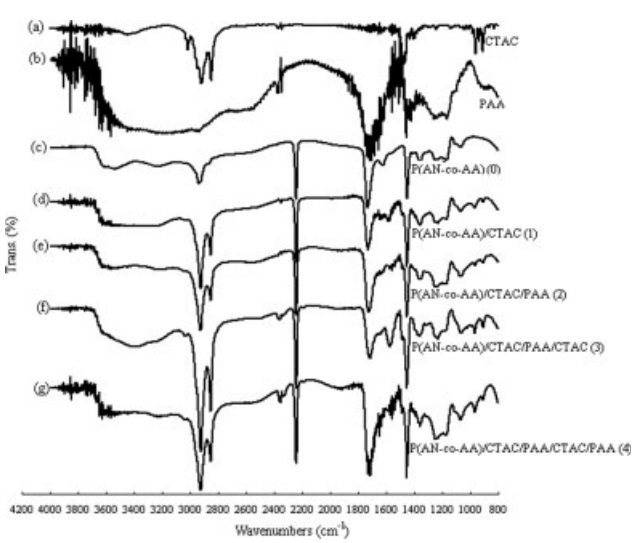

Figure 1 Comparison of the FTIR spectra of the base P(AN-*co*-AA) and the multilayer CTAC/PAA composites on the base P(AN-*co*-AA). The layer numbers of each spectrum are represented as 0, 1, 2, 3, and 4 for P(AN-*co*-AA), P(AN-*co*-AA)/CTAC, P(AN-*co*-AA)/CTAC/PAA, P(AN-*co*-AA)/CTAC/PAA/CTAC, and P(AN-*co*-AA)/CTAC/PAA/CTAC/PAA, respectively.

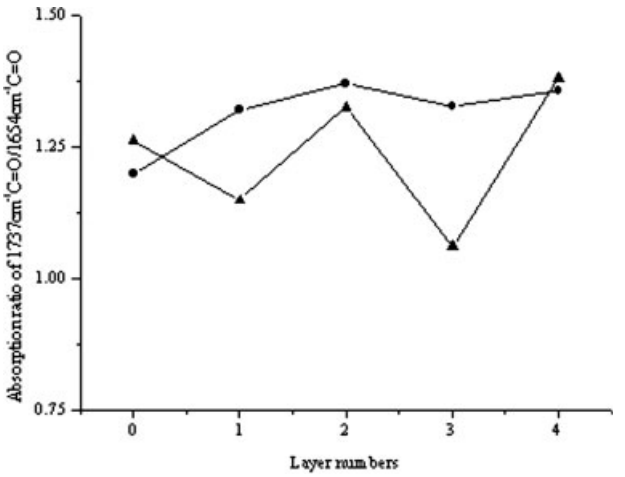

Figure 2 Absorption ratios of the 1737-cm^{-1} C=O band to the 1645-cm^{-1} C=O band assigned to carboxylic acid and the dissociated carboxylic acid, respectively, in the IR spectra obtained for the (▲) P(AN-*co*-AA)/CTAC/PAA and (●) P(AN-*co*-AA)/TMAC/PAA multilayer composites. The layer numbers are the same as those described in Figure 1.

composite layer, the carboxylate peak at 1654 cm^{-1} decreased significantly. This strongly indicated that the interference of dissociation of the carboxylic acid groups of the P(AN-*co*-AA) was caused on the surface. There were tendencies for the C—H absorption at 1454 cm^{-1} to increase with the increasing number of composite layers. Therefore, multilayers of CTAC and PAA were repeatedly formed on the surface of the base polymer.

Relative to amphiphilic CTAC, TMAC contains similar cationic properties except for long alkyl chains on the quaternary ammonium site. The FTIR spectra of the base P(AN-*co*-AA), P(AN-*co*-AA)/TMAC monolayer, and multiple composites having TMAC/PAA on the P(AN-*co*-AA) are shown in Figure 3. Apparently, the dimer band at 3500–2800 cm^{-1} was changed through the formation of the TMAC layer on the P(AN-*co*-AA) and then the PAA layer on the P(AN-*co*-AA)/TMAC. Also, the ratio of ⟩C=O absorption at 1737 cm^{-1} to that of the dissociated carboxylic group at 1645 cm^{-1} increased as the TMAC and PAA were deposited. This was because a part of the dissociated carboxylic group was neutralized with TMAC after the weak base TMAC layer was deposited on the dissociated carboxylic layer of PAA. The FTIR data showed that the C—H absorption around 2920 cm^{-1} increased slightly as the TMAC layer increased. Moreover, the characteristic absorption peak of TMAC around 950 cm^{-1} appeared in the spectra of the following P(AN-*co*-AA)/TMAC/PAA multilayer composites, even though the changes were small relative to P(AN-*co*-AA)/CTAC/PAA.

Surface properties of the base and multilayer composite polymers

To observe the surface morphologies of the ESA layers on the base P(AN-*co*-AA), atomic force microscopy (AFM) was used. Figure 4 shows 20 × 20 μm^2 squares for the surface images of the multilayer composites. To follow the changes in surface morphology, the formation of the CTAC/PAA or TMAC/PAA layers was on the base P(AN-*co*-AA) membrane. Here, the four steps for the preparation of such layers are described as 1, 2, 3, and 4 processes, as described in the Experimental section. By analyzing the AFM data, the surface area of the 20 × 20 μm^2 squares were 401 and 406 μm^2 for cycles 0 and 6, respectively. The surface average height (R_a) of the base P(AN-*co*-AA) layer on the base membrane was about 16 nm. Then, the value indicated that the surface changed to be rough when CTAC and PAA were deposited on the surface (Fig. 5). The CTAC layer deposited by cycle 1 had an R_a of about 24 nm and was lower than those of cycles 3 and 5 for about 29 and 43 nm, respectively. Also, the PAA top layer on the CTAC layer showed R_a's of 35, 48 and 66 nm for cycles 2, 4, and 6, respectively. After the PAA layer was deposited on the CTAC layer, there was tendency toward a rough surface, as shown in the side view of the surface. This tendency was significant when the layer number increased. For example, the value of the average roughness of the P(AN-*co*-AA)/CTAC/PAA/CTAC/PAA/CTAC/PAA layer increased R_a = 66 nm. In comparison with the R_a of the CTAC/PAA system, the TMAC/PAA system showed similar changes through cycles

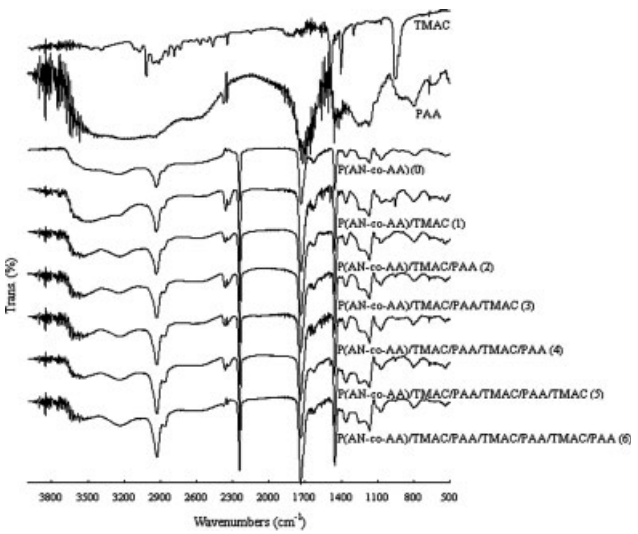

Figure 3 Comparison of the FTIR spectra of the base P(AN-*co*-AA) and P(AN-*co*-AA)/TMAC/PAA multilayer composites. The layer numbers are the same as those described in Figure 1.

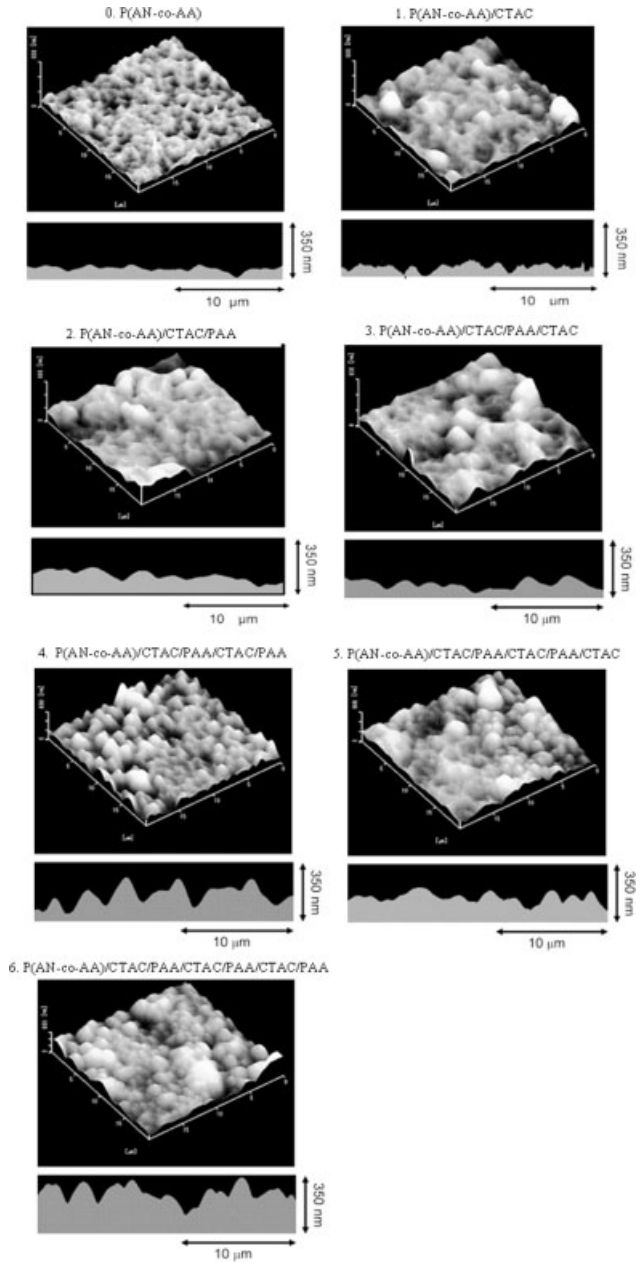

Figure 4 AFM images (20×20 μm^2 square and 600 nm high) for the CTAC/PAA system cycled 0 to 6 in the ESA technique.

1–6, but the R_a value was lower than that of each layer number for the CTAC/PAA system.

To investigate the surface properties of the electrostatic self-assembled surface by CTAC/PAA and TMAC/PAA, the contact angle of water was measured. Here, a water droplet having a volume of 2 μL was on the surface at 25°C. Figure 6 presents values of the contact angles measured for each cycle. We observed that the base P(AN-*co*-AA) surface showed a water contact angel of $60 \pm 2°$. However, after the CTAC layer was deposited on the surface of the base membrane, the value changed to

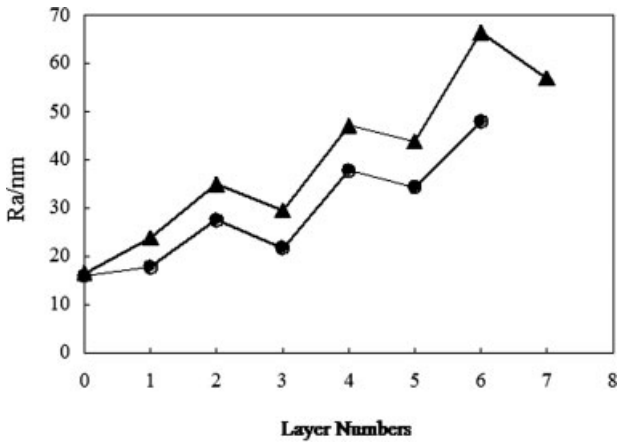

Figure 5 Surface average roughness of the resultant P(AN-*co*-AA) membrane with different numbers of composite layers of CTAC/PAA on the surface.

$70 \pm 1°$ at cycle 1. This meant that CTAC layer was exposed to air on the surface of the membrane. Then, when the PAA layer was formed on the CTAC layer, the value decreased to $58 \pm 2°$, which indicated that the surface nature became much more hydrophilic with the deposition of the PAA layer. Therefore, as shown in Scheme 3 for P(AN-*co*-AA)/CTAC/PAA, the hydrophilic part of the —COOH groups of PAA were exposed to air on the surface and the hydrophobic parts of the main chains of PAA contacted the cetyl layer groups of CTAC. The value of the contact angle again changed, as the CTAC layer was recovered on the PAA layer with similar tendencies in cycles 1 and

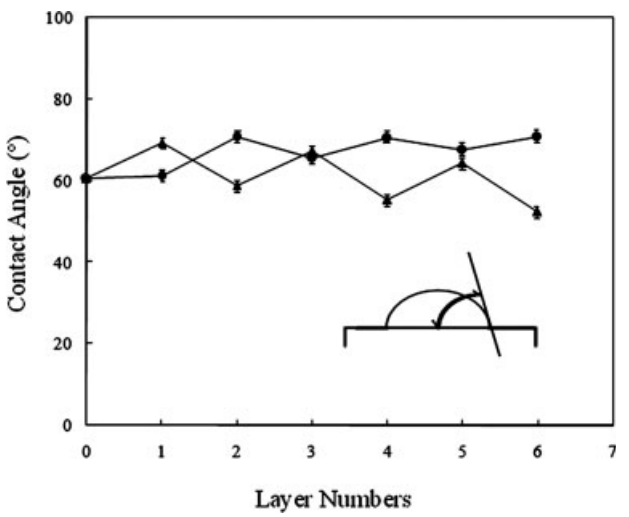

Figure 6 Contact angle of water on the resultant P(AN-*co*-AA) membrane with different numbers of composite layers obtained in (▲) P(AN-*co*-AA)/CTAC/PAA and (●) P(AN-*co*-AA)/TMAC/PAA.

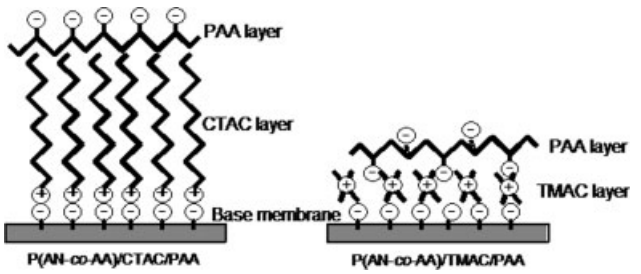

Scheme 3 Illustration images of P(AN-*co*-AA)/CTAC/PAA and P(AN-*co*-AA)/TMAC/PAA layer by layer.

2. As the cycle numbers increased, the values of the contact angle decreased. This indicated that the CTAC and PAA layers deposited alternately on the base P(AN-*co*-AA) surface by the ESA technique. Plotted in Figure 6 are the contact angles when the TMAC and PAA layers were deposited. Less enhancement of the change of the contact angles was observed as TMAC was deposited. However, in cycle 2, the values increased 70 ± 3° and slightly decreased to 66 ± 3° in cycles 3–6. This meant that the PAA layer for cycle 2 electrostatically interacted with the TMAC layer on the P(AN-*co*-AA)/TMAC/PAA membrane. Therefore, the anionic groups of PAA seemed to form ion complex with cationic TMAC and expose the hydrophobic main chains of PAA to the air side.

Application of the multilayer composite surfaces for permeable membranes

As the ESA technique has been applied to prepare several membranes for material separation, high permeability and high separation capability have been achieved for gas and pervaporation.[5–9] However, little has been known about ultrafiltration membranes containing quaternary ammonium salt/polymer anions. In this study, a P(AN-*co*-AA) base membrane was prepared by the phase-inversion method according to our previous studies.[17–19] As shown in Figure 7, scanning electron microscopy (SEM) pictures showed that the membranes used for these experiments had an asymmetric porous structure. This indicated that the membrane had a typical morphology as an ultrafiltration membrane[20,21] and showed a high permeable flux. Because CTAC/PAA multilayers were formed on the base P(AN-*co*-AA), actually, the permeate flux was influenced by the formation layer by layer of CTAC/PAA.

As we expected, the permeability of water through such composite membranes depended on the formation of the ESA layers. After the CTAC or TMAC layer was deposited on the surface of the base P(AN-*co*-AA) membrane, the roughness of the membrane surface decreased when the PAA layer and CTAC or TMAC layer was deposited alternately. Figure 8 shows the changes in volume flux of water passed through the P(AN-*co*-AA) membranes with the layer-by-layer composites. The values of the

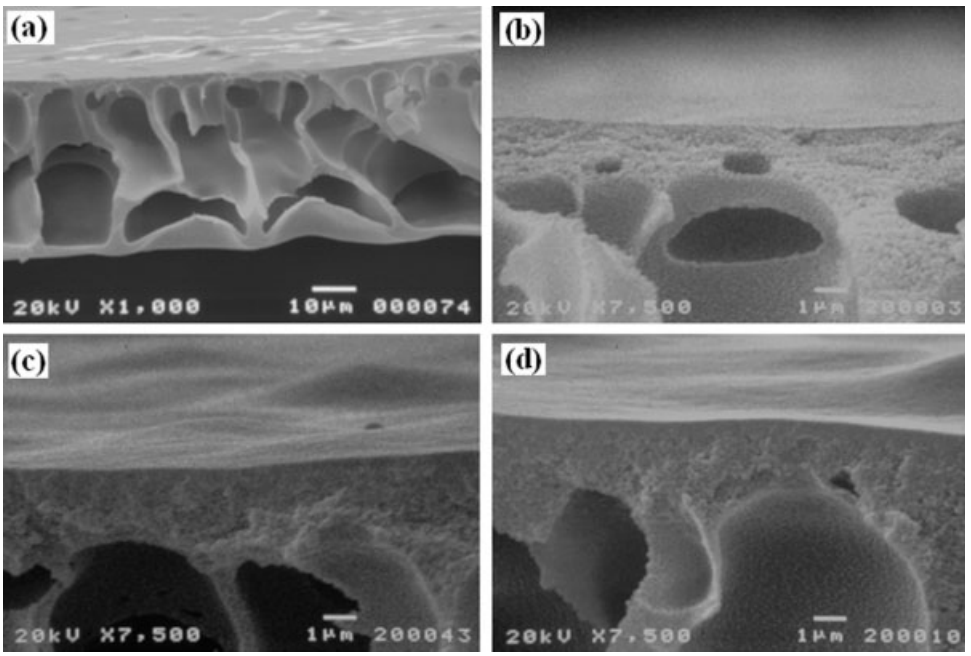

Figure 7 SEM pictures of the (a,b) P(AN-*co*-AA) base membrane, (c) P(AN-*co*-AA)/CTAC monolayer, and (d) P(AN-*co*-AA)/CTAC/PAA multilayer deposited on the base P(AN-*co*-AA) membrane.

water flux decreased as the multilayers formed on the top surface of the membrane. The value of water flux decreased as the first three layers were deposited. Then, cycles of such decreases or increases were observed after layer numbers 3 and 4. In particular for the P(AN-*co*-AA)/CTAC/PAA membrane, when the third and fourth layers were deposited, the value of volume flux of water increased and decreased alternately (Fig. 8). For the P(AN-*co*-AA)/CTAC/PAA membrane, the values of water flux tended to decrease relative to those of P(AN-*co*-AA)/TMAC/PAA. The cause of a such large discrepancy in CTAC/PAA and TMAC/PAA might have been the hydrophobic nature of the quaternary ammonium salt. As shown in Scheme 3, the deposited CTAC layer on the P(AN-*co*-AA) exactly formed a hydrophobic layer made of the aggregated cetyl groups of CTAC on the membrane surface. It is reasonable to consider that such domain formation on the membrane surface disturbed the infiltration of water in P(AN-*co*-AA)/CTAC/PAA.

To determine permeability of PEG and dextran, molecular weight cutoff curves were measured. With different molecular weights of PEG and dextran, we probed the permeability of the resultant membranes. Figure 9 shows the rejection of the base P(AN-*co*-AA) membrane and P(AN-*co*-AA)/CTAC/PAA multilayer membranes to such macromolecular solutes with different molecular weights. The values of rejection increased as the layer numbers increased. The rejection of PEG with a molecular weight of 20,000 and dextran with a molecular weight of 500,000 were about 100% for the P(AN-*co*-AA)/CTAC/PAA/CTAC membrane. This implied that the pore size of the resultant membranes decreased as the multilayers containing CTAC/PAA were formed on the base membrane. Therefore, the

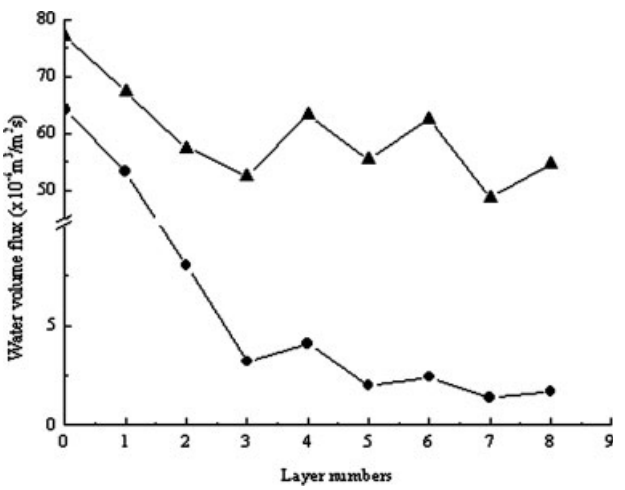

Figure 8 Volume flux of water for the composite membranes containing (●) CTAC/PAA and (▲) TMAC/PAA layers on the base P(AN-*co*-AA) membrane.

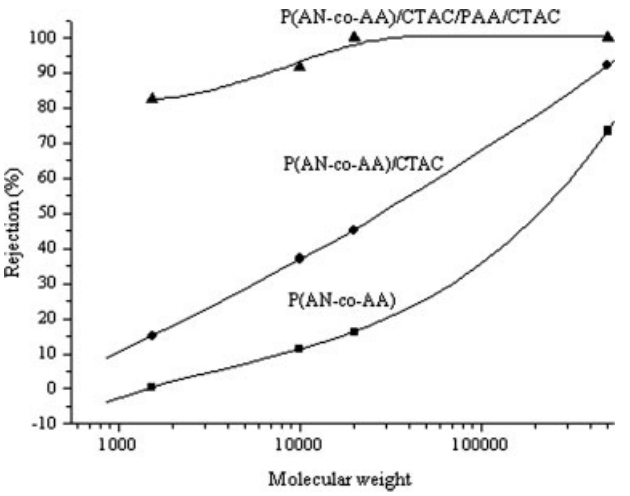

Figure 9 Rejection curves of the (■) base P(AN-*co*-AA), (●) P(AN-*co*-AA)/CTAC, and (▲) P(AN-*co*-AA)/CTAC/PAA/CTAC membranes.

rejection data indicated that the ESA multilayers bridged over the pores of the base P(AN-*co*-AA) membrane. As result, the technique could be applied to control the macromolecular permeability, which indicated that excellent rejection of the permeability of macromolecular solutes was achieved with only a few layers of CTAC/PAA/CTAC on the P(AN-*co*-AA) membrane.

CONCLUSIONS

The surface properties of multilayer composites made of CTAC and PAA were investigated with the ESA technique on a base P(AN-*co*-AA) membrane. FTIR spectroscopy, AFM, SEM, and contact angle techniques were used to evaluate the surfaces. The surface morphology and properties were changed alternately by the formation of multilayers of CTAC/PAA. As an application, the permeability of the resultant membrane also strongly depended upon the formation of the multiple composite layers for water permeability and PEG and dextran rejection. We concluded that this alternative technique has potential for several applications relating to such membrane fields. This would promise reproducible and improved separation membranes. In future studies, the ability of the ESA technique will be studied for the functionalization of metal-ion rejection by such layer-by-layer composites.

References

1. Ulman, A. An Introduction to Ultrathin Organic Films; Academic: Boston, 1991.
2. Fendler, J. H. Membrane-Mimetic Approach to Advanced Materials; Springer-Verlag: Berlin, 1994.
3. Fendler, J. H. Chem Mater 1996, 8, 1616.

4. Decher, G.; Hong, J. D.; Schmitt, J. Thin Solid Films 1992, 832, 210.
5. Toutianoush, A.; Tieke, B. Mater Sci Eng C 2002, 22, 135.
6. Krasemann, L.; Tieke, B. Mater Sci Eng C 1999, 8–9, 513.
7. Stroeve, P.; Vasquez, V.; Cocelho, M. Thin Solid Films 1996, 708, 284.
8. Krasemann, L.; Tieke, B. J Membr Sci 1998, 150, 23.
9. Ackern, F. V.; Krasemann, L.; Tieke, B. Thin Solid Films 1998, 762, 327.
10. Krasemann, L.; Tieke, B. Langmuir 2000, 16, 287.
11. Harris, J. J.; Stair, J. L.; Bruening, M. L. Chem Mater 2000, 12, 1941.
12. Krasemann, L.; Toutianoush, A.; Tieke, B. J Membr Sci 2001, 181, 221.
13. Tieke, B.; Krasemann, L.; Toutianoush, A. Macromol Symp 2001, 163, 97.
14. Haack, J. M.; Lenk, W.; Lehmann, D. J Membr Sci 2001, 184, 233.
15. Zhu, Z. Q.; Feng, X. S.; Penlidis, A. Mater Sci Eng 2006, 26, 1.
16. Won, J.; Chae, S. K.; Kim, J. H. J Membr Sci 2005, 249, 113.
17. Shibata, M.; Kobayashi, T.; Fujii, N. J Appl Polym Sci 2000, 75, 1546.
18. Xia, S. L.; Wang, H. Y.; Kobayashi, T. Mater Res Soc 2004, 787, 103.
19. Wang, H. Y.; Kobayashi, T.; Fujii, N. Langmuir 1996, 12, 4850.
20. Scott, K. Handbook of Industrial Membranes, 2nd ed.; Elsevier Advanced Technology: Oxford, 1998; p 205.
21. Mulder, M. Basic Principles of Membrane Technology; Kluwer Academic: Dordrecht, 1996; p 339.